Electron-, Anion-, and Proton-Transfer Processes Associated with the Redox Chemistry of $Fe(\eta^5\text{-}C_5Ph_5)((\eta^6\text{-}C_6H_5)C_5Ph_4)$ and Its Protonated Form $[Fe(\eta^5\text{-}C_5Ph_5)((\eta^6\text{-}C_6H_5)C_5Ph_4H)]BF_4$ at Microcrystal−Electrode−Solvent (Electrolyte) Interfaces

Alan M. Bond,*[,†] Dirk A. Fiedler,[‡] Axel Lamprecht,[†] and Vanda Tedesco[†]

Department of Chemistry, Monash University, Clayton, Victoria 3168, Australia, and School of Chemistry, La Trobe University, Bundoora, Victoria 3083, Australia

Received September 9, 1998

Voltammograms of microcrystals of $Fe(\eta^5\text{-}C_5Ph_5)((\eta^6\text{-}C_6H_5)C_5Ph_4)$ and $[Fe(\eta^5\text{-}C_5Ph_5)((\eta^6\text{-}C_6H_5)C_5Ph_4H)]BF_4$ mechanically attached to graphite or gold electrodes are well-defined when the electrode is placed in (70:30) water/acetonitrile (0.1 M electrolyte) media. The simplest processes at the electrode−solvent (electrolyte) interface are the chemically reversible oxidation of $Fe(\eta^5\text{-}C_5Ph_5)((\eta^6\text{-}C_6H_5)C_5Ph_4)$, $Fe(\eta^5\text{-}C_5Ph_5)((\eta^6\text{-}C_6H_5)C_5Ph_4)_{(solid)} + X^-_{(solution)} \rightleftharpoons [Fe(\eta^5\text{-}C_5Ph_5)((\eta^6\text{-}C_6H_5)C_5Ph_4)][X]_{(solid)} + e^-$ when X^- is the electrolyte anion (ClO_4^-, BF_4^-, Cl^-, or F^-), and the chemically reversible reduction of $[Fe(\eta^5\text{-}C_5Ph_5)((\eta^6\text{-}C_6H_5)C_5Ph_4H)]BF_4$, $[Fe(\eta^5\text{-}C_5Ph_5)((\eta^6\text{-}C_6H_5)C_5Ph_4H)][BF_4]_{(solid)} + e^- \rightleftharpoons Fe(\eta^5\text{-}C_5Ph_5)((\eta^6\text{-}C_6H_5)C_5Ph_4H)_{(solid)} + BF_4^-{}_{(solution)}$, when BF_4^- is the electrolyte anion. Anion exchange between $BF_4^-{}_{(solid)}$ in $[Fe(\eta^5\text{-}C_5Ph_5)((\eta^6\text{-}C_6H_5)C_5Ph_4H)]BF_4$ and the electrolyte anion, $X^-_{(solution)}$, is rapid so that the potentials of both processes are dependent on the electrolyte anion. Cyclic voltammograms scanned over a potential range encompassing both processes show that interconversion of $[Fe(\eta^5\text{-}C_5Ph_5)((\eta^6\text{-}C_6H_5)C_5Ph_4H)]^+$ and $Fe(\eta^5\text{-}C_5Ph_5)((\eta^6\text{-}C_6H_5)C_5Ph_4)$ occurs when either $[Fe(\eta^5\text{-}C_5Ph_5)((\eta^6\text{-}C_6H_5)C_5Ph_4H)]^+$ or $Fe(\eta^5\text{-}C_5Ph_5)((\eta^6\text{-}C_6H_5)C_5Ph_4)$ is initially present on the electrode surface until ultimately a voltammogram containing responses for both processes is achieved for a given electrolyte. Furthermore, the relative proportion of the two processes is a function of the "pH" of the solution phase, implying that the interfacial reaction $Fe(\eta^5\text{-}C_5Ph_5)((\eta^6\text{-}C_6H_5)C_5Ph_4)_{(solid)} + H^+_{(solution)} + X^-_{(solution)} \rightleftharpoons [Fe(\eta^5\text{-}C_5Ph_5)((\eta^6\text{-}C_6H_5)C_5Ph_4H)][X]_{(solid)}$ is chemically reversible. While interconversion of $Fe(\eta^5\text{-}C_5Ph_5)((\eta^6\text{-}C_6H_5)C_5Ph_4)$ and $[Fe(\eta^5\text{-}C_5Ph_5)((\eta^6\text{-}C_6H_5)C_5Ph_4H)]^+$ is slow, electrochemical oxidation of $Fe(\eta^5\text{-}C_5Ph_5)((\eta^6\text{-}C_6H_5)C_5Ph_4)_{(solid)}$ to $[Fe(\eta^5\text{-}C_5Ph_5)((\eta^6\text{-}C_6H_5)C_5Ph_4)][X]_{2(solid)}$ leads to very rapid formation of $[Fe(\eta^5\text{-}C_5Ph_5)((\eta^6\text{-}C_6H_5)C_5Ph_4H)][X]_{(solid)}$, possibly via the reaction scheme $Fe(\eta^5\text{-}C_5Ph_5)((\eta^6\text{-}C_6H_5)C_5Ph_4)_{(solid)} + X^-_{(solution)} \rightleftharpoons [Fe(\eta^5\text{-}C_5Ph_5)((\eta^6\text{-}C_6H_5)C_5Ph_4)][X]_{(solid)} + e^-$; $[Fe(\eta^5\text{-}C_5Ph_5)((\eta^6\text{-}C_6H_5)C_5Ph_4)][X]_{(solid)} + X^-_{(solution)} \rightleftharpoons [Fe(\eta^5\text{-}C_5Ph_5)((\eta^6\text{-}C_6H_5)C_5Ph_4)][X]_{2(solid)} + e^-$; $2[Fe(\eta^5\text{-}C_5Ph_5)((\eta^6\text{-}C_6H_5)C_5Ph_4)][X]_{2(solid)} + 2H_2O \rightarrow 2[Fe(\eta^5\text{-}C_5Ph_5)((\eta^6\text{-}C_6H_5)C_5Ph_4H)][X]_{(solid)} + O_{2(solution)} + 2H^+_{(solution)} + 2X^-_{(solution)}$. However, the possible involvement of radical-based pathways in the conversion of $[Fe(\eta^5\text{-}C_5Ph_5)((\eta^6\text{-}C_6H_5)C_5Ph_4)][X]_{2(solid)}$ to $[Fe(\eta^5\text{-}C_5Ph_5)((\eta^6\text{-}C_6H_5)C_5Ph_4H)][X]_{(solid)}$ cannot be excluded. An additional process, which is believed to be ligand based, is observed at a very positive potential. Electrospray mass spectrometric data confirm that $[Fe(\eta^5\text{-}C_5Ph_5)((\eta^6\text{-}C_6H_5)C_5Ph_4)]^+$ is a product of oxidation of the parent compound and that conversion of both $Fe(\eta^5\text{-}C_5Ph_5)((\eta^6\text{-}C_6H_5)C_5Ph_4)_{(solid)}$ and its cation to $[Fe(\eta^5\text{-}C_5Ph_5)((\eta^6\text{-}C_6H_5)C_5Ph_4H)]X_{(solid)}$ occurs, while the electrochemical quartz crystal microbalance data verify that anion transport across the electrode−solid−solvent (electrolyte) interface accompanies the electron- and proton-transfer reactions, thereby achieving charge neutralization.

Introduction

In the past few years there has been considerable interest in the interfacial chemistry associated with reactions involving solids. A wide range of voltammetric methods have been developed to facilitate studies of the electron transport and charge transport processes that occur at solid−electrode−solvent interfaces.[1]

In this paper, we report the results of an investigation of the redox and proton-transfer processes that occur when microcrystals of $Fe(\eta^5\text{-}C_5Ph_5)((\eta^6\text{-}C_6H_5)C_5Ph_4)$ (structure 1) and $[Fe(\eta^5\text{-}C_5Ph_5)((\eta^6\text{-}C_6H_5)C_5Ph_4H)]^+$ (structure 2) are mechanically attached to electrodes that are placed in a (70:30) water/acetonitrile medium containing a range of electrolytes. Unlike earlier studies from these laboratories in which the redox chemistry of microcrys-

[†] Monash University.
[‡] La Trobe University.

(1) Scholz, F.; Meyer, B. *Chem. Soc. Rev.* **1994**, *23*, 341, and references therein.

10.1021/om9807553 CCC: $18.00
Publication on Web 01/29/1999

tals of organic, organometallic, and inorganic compounds (see refs 2−8 for example) has been studied at the solid−electrode−solvent (electrolyte) interface, this redox system provides the possibility of both proton and electrolyte ion transfer as well as electron transfer. To unravel the different interfacial processes that occur in these systems, a range of voltammetric and other techniques have been employed.

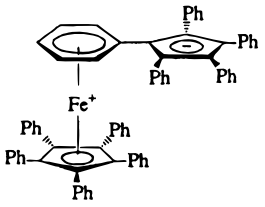

Structure 1

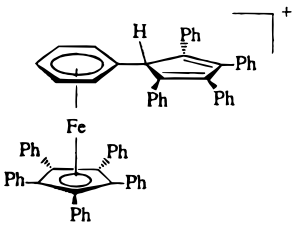

Structure 2

Experimental Section

Solid samples of Fe(η^5-C_5Ph_5)((η^6-C_6H_5)C_5Ph_4), [Fe(η^5-C_5Ph_5)((η^6-C_6H_5)C_5Ph_4H)]BF_4, and 1,2,3,4,5-pentaphenylcyclopentadiene (HC_5Ph_5) were prepared as described in the literature.[9−11] The samples were thoroughly dried prior to use to ensure no solvent was present in the sample. Distilled water and HPLC grade acetonitrile were used for the preparation of the mixed water/acetonitrile solution, and all electrolytes were of analytical or electrochemical grade purity.

Electrochemical experiments were carried out at room temperature (20 ± 2 °C) with a BAS 100 electrochemical analyzer (Bioanalytical Systems, West Lafayette, IN). The reference electrode was Ag/AgCl (3 M NaCl), and the auxiliary electrode was a platinum wire. The reference electrode was calibrated using the $[Fe(CN)_6]^{4-/3-}$ couple in aqueous 1 M KCl, and the reversible half-wave potential for this redox process was found to be 259 ± 3 mV vs Ag/AgCl (3 M NaCl). All potentials reported in this paper are given relative to this Ag/AgCl (3 M NaCl) reference electrode. In most voltammetric experiments a basal plane pyrolytic graphite electrode (5 mm diameter) was used as the working electrode. The electroactive compound was transferred to the surface of the carbon electrode by placing a small amount of the solid material on a coarse grade filter paper and then rubbing the carbon electrode over the compound, thereby causing some of the compound to adhere to the electrode surface. The electrode to which the sample was attached was then placed into the solvent (electrolyte) medium, which had been thoroughly purged with nitrogen to remove oxygen. Experiments undertaken at gold working electrodes showed results analogous to those found with the basal plane pyrolytic graphite electrode. However, the signal-to-background current ratio was more favorable with the pyrolytic graphite electrode.

Electrospray mass spectra (ESMS) were recorded in the positive ion detection mode using a Micromass Platform II quadrupole spectrometer. Cone voltages were the minimum necessary (15−30 V), and the solution flow rate was 5 μL min^{-1}. Samples for examination by ESMS were prepared by dissolution in pure acetonitrile of solids attached to the electrode surface, which had been in contact with the (70:30) water/acetonitrile solution.

An ELCHEMA electrochemical quartz crystal microbalance (EQCN-701, Potsdam, NY) with 10 MHz AT-cut quartz crystals (Bright Star Crystal Pty. Ltd., Vermont, Victoria 3133, Australia) was used for the simultaneous cyclic voltammetric and mass balance experiments. The quartz crystals were coated with 5 mm diameter gold electrodes. The method developed by Deakin and Melroy[12] was employed to calibrate the quartz crystal microbalance using a 0.01 M $CuSO_4$ solution in 0.1 M HNO_3. A uniform distribution of Fe(η^5-C_5Ph_5)((η^6-C_6H_5)C_5Ph_4) and [Fe(η^5-C_5Ph_5)((η^6-C_6H_5)C_5Ph_4H)]BF_4 on the gold electrode was obtained by rubbing the solid over the electrode surface with a cotton bud.

"pH"-measurements were performed on a model 900P pH-meter from TPS Pty. Ltd., Brisbane, Australia.

Results and Discussion

Fe(η^5-C_5Ph_5)((η^6-C_6H_5)C_5Ph_4) and [Fe(η^5-C_5Ph_5)((η^6-C_6H_5)C_5Ph_4H)]BF_4 are both insoluble in water. Consequently, it was anticipated that the solid-state voltammetry of microcrystals of these compounds could have been examined at the microcrystal−electrode−water (electrolyte) interface as was the case with the related decamethylferrocene compounds Fe(η^5-C_5Me_5)$_2$ and [Fe(η^5-C_5Me_5)$_2$]BF_4.[4b] However, no well-defined voltammetric response was obtained for Fe(η^5-C_5Ph_5)((η^6-C_6H_5)C_5Ph_4) and [Fe(η^5-C_5Ph_5)((η^6-C_6H_5)C_5Ph_4H)]BF_4 mechanically attached to a basal plane pyrolytic graphite or gold electrode placed into aqueous (electrolyte) solution. In contrast, when a (70:30) water/acetonitrile (electrolyte) solvent mixture was used, very strong signals could be obtained, and this mixed solvent rather than a purely aqueous medium was chosen for the investigation.

Voltammetry of Microcrystals of [Fe(η^5-C_5Ph_5)((η^6-C_6H_5)C_5Ph_4H)]BF_4 Mechanically Attached to a Graphite Electrode Placed in (70:30) Water/Acetonitrile (Electrolyte). (i) Reduction of [Fe(η^5-C_5Ph_5)((η^6-C_6H_5)C_5Ph_4H)]BF_4. A cyclic voltammogram of [Fe(η^5-C_5Ph_5)((η^6-C_6H_5)C_5Ph_4H)]BF_4 mechanically attached to a basal plane pyrolytic graphite electrode, which is then immersed in (70:30) water/acetonitrile containing 0.1 M $NaClO_4$ as the electrolyte, is shown in Figure 1a over the potential range of 0.5 to −1.2 V at a scan rate of 200 mV s^{-1}. A very well-defined chemically reversible couple having reduction (E_p^{red}) and oxidation (E_p^{ox}) peak potentials at $E_p^{red} = -935$ mV and $E_p^{ox} = -820$ mV is observed. Both the peak widths and peak potentials are a function of scan rate. At higher scan rates, the signals broaden and the peak-to-peak separation increases from 45 mV at 10 mV s^{-1} to 145 mV at 500 mV s^{-1}. The areas (charge) associated with the reduction and oxidation component of the voltammogram are equal within experimental error (±2%). This reduction step can be assigned to the process given

(2) Bond, A. M.; Scholz, F. (a) *J. Phys. Chem.* **1991**, *95*, 7640; (b) *Langmuir* **1991**, *7*, 3197; (c) *J. Geochem. Expl.* **1992**, *42*, 227.
(3) Dueber, R. E.; Bond, A. M.; Dickens, P. G. *J. Electrochem. Soc.* **1992**, *139*, 2363.
(4) (a) Bond, A. M.; Colton, R.; Daniels, F.; Fernando, D. R.; Marken, F.; Nagaosa, Y.; Van Steveninck, R. F. M.; Walter, J. N. *J. Am. Chem. Soc.* **1993**, *115*, 9556. (b) Bond, A. M.; Marken, F. *J. Electroanal. Chem.* **1994**, *372*, 125. (c) Bond, A. M.; Colton, R.; Marken, F.; Walter, J. N. *Organometallics* **1994**, *13*, 5122. (d) Dostal, A.; Meyer, B.; Scholz, F.; Schröder, U.; Bond, A. M.; Marken, F.; Shaw, S. J. *J. Phys. Chem.* **1995**, *99*, 2096. (e) Bond, A. M.; Cooper, J. B.; Marken, F.; Way, D. M. *J. Electroanal. Chem.* **1995**, *396*, 407. (f) Downard, A. J.; Bond, A. M.; Hanton, L. R.; Heath, G. A. *Inorg. Chem.* **1995**, *34*, 6387.
(5) Dostal, A.; Schröder, U.; Scholz, F. *Inorg. Chem.* **1995**, *34*, 1711.
(6) Komorsky-Lovric, Š. *J. Electroanal. Chem.* **1995**, *397*, 211.
(7) Shaw, S. J.; Marken, F.; Bond, A. M. (a) *J. Electroanal. Chem.* **1996**, *404*, 227; (b) *Electroanalysis* **1996**, *8*, 732.
(8) Bond, A. M.; Fletcher, S.; Marken, F.; Shaw, S. J.; Symons, P. G. *J. Chem. Soc., Faraday Trans.* **1996**, *92*, 3925, and references therein.
(9) Schumann, H.; Lentz, A.; Weimann, R.; Pickardt, J. *Angew. Chem.* **1994**, *106*, 1827; *Angew. Chem., Int. Ed. Engl.* **1994**, *33*, 1731.
(10) Brown, K. N.; Field, L. D.; Lay, P. A.; Lindall, C. M.; Masters, A. F. *J. Chem. Soc., Chem. Commun.* **1990**, 408.
(11) Field, L. D.; Ho, K. M.; Lindall, C. M.; Masters, A. F.; Webb, A. G. *Aust. J. Chem.* **1990**, *43*, 281.
(12) Deakin, M. R.; Melroy, O. *J. Electroanal. Chem.* **1988**, *239*, 321.

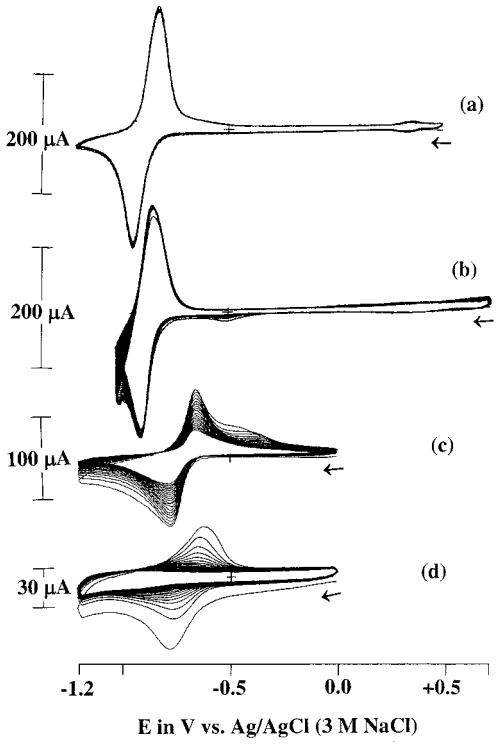

Figure 1. Cyclic voltammograms obtained at a scan rate of 200 mV s^{-1} for $[Fe(\eta^5\text{-}C_5Ph_5)((\eta^6\text{-}C_6H_5)C_5Ph_4H)]BF_4$ mechanically attached to a basal plane pyrolytic graphite electrode placed in (70:30) water/acetonitrile. Electrolytes are (a) 0.1 M $NaClO_4$, (b) 0.1 M $HClO_4$, (c) 0.1 M NaCl, and (d) 0.1 M NaF.

in eq 1, assuming that the BF_4^- anion initially present in the solid has been exchanged for the electrolyte anion ClO_4^-, prior to commencing the voltammetric experiments.

$$[Fe(\eta^5\text{-}C_5Ph_5)((\eta^6\text{-}C_6H_5)C_5Ph_4H)]ClO_{4(solid)} + e^- \rightleftharpoons Fe(\eta^5\text{-}C_5Ph_5)((\eta^6\text{-}C_6H_5)C_5Ph_4H)_{(solid)} + ClO_4^-{}_{(solution)} \quad (1)$$

In dichloromethane,[13] the equivalent solution-phase reversible process, which is described by eq 2, has been observed.

$$[Fe(\eta^5\text{-}C_5Ph_5)((\eta^6\text{-}C_6H_5)C_5Ph_4H)]^+_{(solution)} + e^- \rightleftharpoons Fe(\eta^5\text{-}C_5Ph_5)((\eta^6\text{-}C_6H_5)C_5Ph_4H)_{(solution)} \quad (2)$$

Close inspection of Figure 1a reveals the presence of a second chemically reversible couple at $E_p^{ox} = 345$ mV and $E_p^{red} = 340$ mV. It will be proved via data provided below that this process can be assigned to the oxidation and reduction of $Fe(\eta^5\text{-}C_5Ph_5)((\eta^6\text{-}C_6H_5)C_5Ph_4)$, as in eq 3.

$$Fe(\eta^5\text{-}C_5Ph_5)((\eta^6\text{-}C_6H_5)C_5Ph_4)_{(solid)} + ClO_4^-{}_{(solution)} \rightleftharpoons [Fe(\eta^5\text{-}C_5Ph_5)((\eta^6\text{-}C_6H_5)C_5Ph_4)]ClO_{4(solid)} + e^- \quad (3)$$

The dichloromethane solution-phase voltammetry of $Fe(\eta^5\text{-}C_5Ph_5)((\eta^6\text{-}C_6H_5)C_5Ph_4)$[13] is complicated by structural rearrangements to the $Fe(\eta^5\text{-}C_5Ph_5)_2$ symmetrical isomer as well as acid−base reactions, but the analogous solution-phase process (eq 4) has been identified.

$$Fe(\eta^5\text{-}C_5Ph_5)((\eta^6\text{-}C_6H_5)C_5Ph_4)_{(solution)} \rightleftharpoons [Fe(\eta^5\text{-}C_5Ph_5)((\eta^6\text{-}C_6H_5)C_5Ph_4)]^+_{(solution)} + e^- \quad (4)$$

On cycling the potential over a range that encompasses both processes, it was observed initially that the peak currents of the $[Fe(\eta^5\text{-}C_5Ph_5)((\eta^6\text{-}C_6H_5)C_5Ph_4H)]^{+/0}$ redox couple slightly decrease, while the peak currents for the $[Fe(\eta^5\text{-}C_5Ph_5)((\eta^6\text{-}C_6H_5)C_5Ph_4)]^{+/0}$ couple slightly increase. However, after a few cycles of the potential a constant voltammetric response is reached, in which the magnitudes of the peak currents of the $[Fe(\eta^5\text{-}C_5Ph_5)((\eta^6\text{-}C_6H_5)C_5Ph_4)]^{+/0}$ couple are always very small relative to those for the $[Fe(\eta^5\text{-}C_5Ph_5)((\eta^6\text{-}C_6H_5)C_5Ph_4H)]^{+/0}$ redox couple. The measured "pH-value" of the (70:30) water/acetonitrile (0.1 M $NaClO_4$) solution is 7.2. A significant increase of the peak current for the $[Fe(\eta^5\text{-}C_5Ph_5)((\eta^6\text{-}C_6H_5)C_5Ph_4)]^{+/0}$ redox couple was observed by increasing the measured "pH-value" to 11.0 by addition of NaOH. Conversely the magnitude of this process can be decreased by addition of acid to the mixed solvent medium, with this process not being detectable at "pH" = 5.0. The presence of $Fe(\eta^5\text{-}C_5Ph_5)((\eta^6\text{-}C_6H_5)C_5Ph_4)$ on the electrode surface therefore may be attributed to the equilibrium reaction

$$[Fe(\eta^5\text{-}C_5Ph_5)((\eta^6\text{-}C_6H_5)C_5Ph_4H)][ClO_4]_{(solid)} \rightleftharpoons Fe(\eta^5\text{-}C_5Ph_5)((\eta^6\text{-}C_6H_5)C_5Ph_4)_{(solid)} + H^+_{(solution)} + ClO_4^-{}_{(solution)} \quad (5)$$

with the equilibrium position lying far to the left when the solids are in contact with neutral aqueous media.

The peak potentials for the $[Fe(\eta^5\text{-}C_5Ph_5)((\eta^6\text{-}C_6H_5)C_5Ph_4H)]^{+/0}$ redox couple are independent of whether 0.1 M $HClO_4$ or 0.1 M $NaClO_4$ is used as the electrolyte (Table 1), implying that the nature of the cation is not significant. In contrast the redox couple is observed at less negative values when 0.1 M KBF_4 is the electrolyte (Table 1). This latter result supports the hypothesis that the BF_4^- anion had been replaced by ClO_4^- in studies where a perchlorate electrolyte is present. Furthermore, with the strongly acidic 0.1 M $HClO_4$ electrolyte ("pH" = 1.0) or 0.1 M KBF_4 ("pH" = 5.0) as the electrolyte, the redox couple associated with the oxidation of the unprotonated form $Fe(\eta^5\text{-}C_5Ph_5)((\eta^6\text{-}C_6H_5)C_5Ph_4)$ is not observed (Figure 1b) since the proton concentration is now sufficiently high to prevent deprotonation of $[Fe(\eta^5\text{-}C_5Ph_5)((\eta^6\text{-}C_6H_5)C_5Ph_4H)]BF_4$ from occurring to any significant extent. The acidity associated with the 0.1 M KBF_4 solution ("pH" = 5.0) presumably is associated with hydrolysis of BF_4^- to give low concentrations of boric acid. In the presence of 0.1 M $HClO_4$, a small process that has potentials of $E_p^{red} = -510$ mV and $E_p^{ox} = -485$ mV is observed prior to the major process (see Figure 1b). The equivalent process is barely detectable at $E_p^{red} = -345$ or -500 mV when 0.1 M KBF_4 or $NaClO_4$ is the electrolyte (Table 1). However, the identity of the complex giving rise to this process and the mechanism of the reaction are unknown.

(13) Bond, A. M.; Colton, R.; Fiedler, D. A.; Field, L. D.; He, T.; Humphrey, P. A.; Lindall, C. M.; Marken, F.; Masters, A. F.; Schumann, H.; Sühring, K.; Tedesco, V. *Organometallics* **1997**, *16*, 2787.

Table 1. Cyclic Voltammetric Data Obtained for the Primary Processes for Reduction of [Fe(η^5-C_5Ph_5)((η^6-C_6H_5)C_5Ph_4H)]BF_4 and Oxidation of Fe(η^5-C_5Ph_5)((η^6-C_6H_5)C_5Ph_4) Mechanically Attached to a Basal Plane Pyrolytic Graphite Electrode Immersed in (70:30) Water/Acetonitrile (0.1 M Electrolyte)[a]

starting material	electrolyte[b] (0.1 M)	E_p^{ox} (mV)	E_p^{red} (mV)	($E_p^{ox} - E_p^{red}$) (mV)	E_p^{red} or E_p^{ox} [d] (mV)
[Fe(η^5-C_5Ph_5)((η^6-C_6H_5)C_5Ph_4H)]BF_4	$NaClO_4$ (7.2)	−820	−935	115	−500
	$HClO_4$ (1.0)	−870	−930	60	−510/−485
	KBF_4 (5.0)	−810	−890	80	−345
	NaCl (6.4)	−665	−765	100	
	NaF (7.7)	−640	−760	120	
Fe(η^5-C_5Ph_5)((η^6-C_6H_5)C_5Ph_4)	$NaClO_4$ (7.2)	420	345	75	−500
	$HClO_4$ (1.0)	405	365	40	−500
	KBF_4 (5.0)	445	400	45	
	NaCl (6.4)	550 (530)[c]	525	25	
	NaF (7.7)	625 (560)[c]	520	105	

[a] $T = 20 \pm 2$ °C, scan rate = 200 mV s^{-1}, potentials reported versus Ag/AgCl (3 M NaCl). [b] "pH-values" of the electrolyte are in parentheses. [c] Value of E_p^{ox} from second cycle onward. [d] Weak irreversible reduction process only observed in 0.1 M $NaClO_4$, $HClO_4$, and KBF_4.

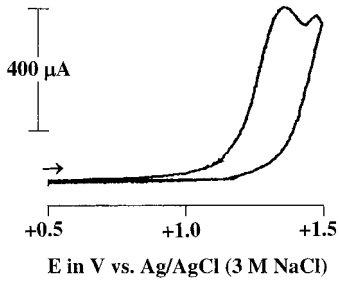

Figure 2. Cyclic voltammograms obtained at a scan rate of 200 mV s^{-1} for oxidation of [Fe(η^5-C_5Ph_5)((η^6-C_6H_5)C_5Ph_4H)]BF_4 mechanically attached to a basal plane pyrolytic graphite electrode placed in (70:30) water/acetonitrile (0.1 M $NaClO_4$).

When 0.1 M NaCl or NaF is used as the electrolyte, the peak potentials for the chemically reversible reduction process are shifted to considerably less negative potentials than those obtained with 0.1 M $NaClO_4$, $HClO_4$, and KBF_4 (Table 1). However, with the halides, the peak currents steadily decrease on cycling of the potential (Figure 1c,d). This time dependence suggests that when insoluble [Fe(η^5-C_5Ph_5)((η^6-C_6H_5)C_5Ph_4H)]BF_4 is in contact with 0.1 M NaCl or 0.1 M NaF electrolyte, ion-exchange processes occur to generate [Fe(η^5-C_5Ph_5)((η^6-C_6H_5)C_5Ph_4H)]Cl and [Fe(η^5-C_5Ph_5)((η^6-C_6H_5)C_5Ph_4H)]F, respectively, which are sparingly soluble in the water/acetonitrile solvent mixture. The [Fe(η^5-C_5Ph_5)((η^6-C_6H_5)C_5Ph_4)]$^{+/0}$ redox couple is again detected when 0.1 M NaCl is the electrolyte ("pH" = 6.4). Interestingly, the peak currents for the [Fe(η^5-C_5Ph_5)((η^6-C_6H_5)C_5Ph_4)]$^{+/0}$ redox couple diminish slower than the peak currents for the [Fe(η^5-C_5Ph_5)((η^6-C_6H_5)C_5Ph_4H)]$^{+/0}$ redox couple and are still visible after the [Fe(η^5-C_5Ph_5)((η^6-C_6H_5)C_5Ph_4H)]$^{+/0}$ couple has disappeared. This result implies that [Fe(η^5-C_5Ph_5)((η^6-C_6H_5)C_5Ph_4H)]Cl is more soluble in the (70:30) water/acetonitrile solvent mixture than [Fe(η^5-C_5Ph_5)((η^6-C_6H_5)C_5Ph_4)]Cl, which is consistent with the observation made in the experiments with Fe(η^5-C_5Ph_5)((η^6-C_6H_5)C_5Ph_4) in 0.1 M NaCl electrolyte solution (see below).

(ii) Oxidation of [Fe(η^5-C_5Ph_5)((η^6-C_6H_5)C_5Ph_4H)]BF_4. [Fe(η^5-C_5Ph_5)((η^6-C_6H_5)C_5Ph_4H)]BF_4 may be irreversibly oxidized at potentials around $E_p^{ox} = 1300$ mV (Figure 2). With cycling of the potential, several new irreversible reduction and oxidation waves appear in the second and third cycles. However, all peak currents decrease in the subsequent cycles of the potential presumably because of the dissolution of the products formed after oxidation of [Fe(η^5-C_5Ph_5)((η^6-C_6H_5)C_5Ph_4H)]$^+$. In the second cycle, the strong oxidation peak at $E_p^{ox} = 1355$ mV is no longer observed. The reduction and oxidation potentials with 0.1 M $NaClO_4$ as the electrolyte are given in Table 2. Comparison with data obtained for oxidation of HC_5Ph_5 (see later discussion and data in Table 2) suggests that oxidation of [Fe(η^5-C_5Ph_5)((η^6-C_6H_5)C_5Ph_4H)]$^+$ may be a ligand-based rather than metal-based process.

Voltammetry of Microcrystals of Fe(η^5-C_5Ph_5)((η^6-C_6H_5)C_5Ph_4) Mechanically Attached to a Graphite Electrode Placed in (70:30) Water/Acetonitrile (0.1 M Electrolyte). (i) Oxidation of Fe(η^5-C_5Ph_5)((η^6-C_6H_5)C_5Ph_4). Figure 3a shows cyclic voltammograms obtained when Fe(η^5-C_5Ph_5)((η^6-C_6H_5)C_5Ph_4) is attached to a basal plane pyrolytic graphite electrode immersed in 0.1 M $NaClO_4$ solution and the potential is scanned over the potential range of 700 to −1200 mV. Initially, only a single chemically reversible redox couple is observed ($E_p^{ox} = 420$ and $E_p^{red} = 345$ mV), which corresponds to the minor process previously reported in voltammetric studies of [Fe(η^5-C_5Ph_5)((η^6-C_6H_5)C_5Ph_4H)]BF_4 (eq 3). On cycling the potential, the chemically reversible redox couple, which grows at $E_p^{red} = -945$ and $E_p^{ox} = -760$ mV, has peak potentials and other voltammetric characteristics that are very similar to those reported previously for the [Fe(η^5-C_5Ph_5)((η^6-C_6H_5)C_5Ph_4H)]$^{+/0}$ process. Consequently, this new redox couple is associated with the formation and then reduction of [Fe(η^5-C_5Ph_5)((η^6-C_6H_5)C_5Ph_4H)]$^+$ to Fe(η^5-C_5Ph_5)((η^6-C_6H_5)C_5Ph_4H). At slow scan rates, the detection of the [Fe(η^5-C_5Ph_5)((η^6-C_6H_5)C_5Ph_4H)]$^{+/0}$ redox couple required fewer cycles of potential than was the case when higher scan rates were employed. Furthermore, when the potential was only cycled over potential regions where Fe(η^5-C_5Ph_5)((η^6-C_6H_5)C_5Ph_4) is not oxidized, the magnitude of the [Fe(η^5-C_5Ph_5)((η^6-C_6H_5)C_5Ph_4H)]$^{+/0}$ redox couple still increased as a function of time. This result shows that protonation does not require the oxidation of Fe(η^5-C_5Ph_5)((η^6-C_6H_5)C_5Ph_4) to [Fe(η^5-C_5Ph_5)((η^6-C_6H_5)C_5Ph_4)]$^+$. That is, the reaction

$$\text{Fe}(\eta^5\text{-C}_5\text{Ph}_5)((\eta^6\text{-C}_6\text{H}_5)\text{C}_5\text{Ph}_4)_{(\text{solid})} + \text{ClO}_4^-{}_{(\text{solution})} + \text{H}^+{}_{(\text{solution})} \rightleftharpoons [\text{Fe}(\eta^5\text{-C}_5\text{Ph}_5)((\eta^6\text{-C}_6\text{H}_5)\text{C}_5\text{Ph}_4\text{H})][\text{ClO}_4]_{(\text{solid})} \quad (6)$$

Table 2. Cyclic Voltammetric Data[a] Obtained for the Oxidation of [Fe(η^5-C_5Ph_5)((η^6-C_6H_5)C_5Ph_4H)]BF_4 and HC_5Ph_5 Mechanically Attached to a Basal Plane Pyrolytic Graphite Electrode Immersed in (70:30) Water/Acetonitrile (0.1 M $NaClO_4$)

starting material	E_p^{ox} (mV)	E_p^{red} (mV)
[Fe(η^5-C_5Ph_5)((η^6-C_6H_5)C_5Ph_4H)]BF_4	1355,[b] 260, 920, 1115	−460, −1150
HC_5Ph_5	1370,[c] 630, 930, 1130	−620, −1090, −1450

[a] $T = 20 \pm 2$ °C, scan rate = 200 mV s^{-1}, potentials reported versus Ag/AgCl (3 M NaCl). [b] Irreversible oxidation wave of [Fe(η^5-C_5Ph_5)((η^6-C_6H_5)C_5Ph_4H)]BF_4. [c] Irreversible oxidation wave of HC_5Ph_5.

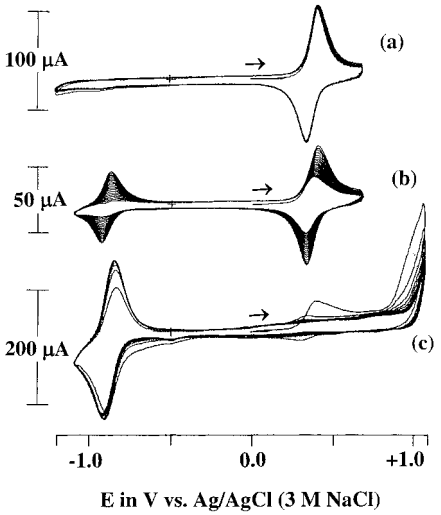

Figure 3. Cyclic voltammograms obtained at a scan rate of 200 mV s^{-1} for Fe(η^5-C_5Ph_5)((η^6-C_6H_5)C_5Ph_4) mechanically attached to a basal plane pyrolytic graphite electrode placed in (70:30) water/acetonitrile. Electrolytes are (a and c) 0.1 M $NaClO_4$ and (b) 0.1 M $HClO_4$.

occurs spontaneously in both directions (see also eq 5) until an equilibrium position is achieved at the solid−solvent (electrolyte) interface so that after a period of time voltammograms commencing with either Fe(η^5-C_5Ph_5)((η^6-C_6H_5)C_5Ph_4) or [Fe(η^5-C_5Ph_5)((η^6-C_6H_5)C_5Ph_4H)]BF_4 contain two chemically reversible processes corresponding to oxidation of Fe(η^5-C_5Ph_5)((η^6-C_6H_5)C_5Ph_4) and reduction of [Fe(η^5-C_5Ph_5)((η^6-C_6H_5)C_5Ph_4H)]$^+$.

With acidic 0.1 M $HClO_4$ as the electrolyte ("pH" = 1.0), the conversion of neutral Fe(η^5-C_5Ph_5)((η^6-C_6H_5)C_5Ph_4) to [Fe(η^5-C_5Ph_5)((η^6-C_6H_5)C_5Ph_4H)]$^+$ is very much faster than when 0.1 M $NaClO_4$ ("pH" = 7.2) is present (Figure 3b). That is, the [Fe(η^5-C_5Ph_5)((η^6-C_6H_5)C_5Ph_4)]$^{+/0}$ redox couple is rapidly and completely converted to the [Fe(η^5-C_5Ph_5)((η^6-C_6H_5)C_5Ph_4H)]$^{+/0}$ couple. With 0.1 M KBF_4 as the electrolyte, the conversion is slower than with 0.1 M $HClO_4$ but faster than with 0.1 M $NaClO_4$ as the electrolyte. Whereas the redox potentials in 0.1 M $NaClO_4$ and $HClO_4$ are the same for the oxidation and reduction of Fe(η^5-C_5Ph_5)((η^6-C_6H_5)C_5Ph_4), in 0.1 M KBF_4, the potentials are shifted to more positive values (Table 1).

With 0.1 M NaCl as the electrolyte, slow dissolution of the chloride salt [Fe(η^5-C_5Ph_5)((η^6-C_6H_5)C_5Ph_4)]Cl occurs on cycling the potential at a scan rate of 200 mV s^{-1} over the potential range of the initial [Fe(η^5-C_5Ph_5)((η^6-C_6H_5)C_5Ph_4)]$^{+/0}$ process, while the [Fe(η^5-C_5Ph_5)((η^6-C_6H_5)C_5Ph_4H)]$^{+/0}$ redox couple is observed to be only very weak. The dissolution rate is even faster when 0.1 M NaF is the electrolyte. The very weak detectable or missing [Fe(η^5-C_5Ph_5)((η^6-C_6H_5)C_5Ph_4H)]$^{+/0}$ redox couple in 0.1 M NaCl and NaF, respectively, may be explained by assuming that [Fe(η^5-C_5Ph_5)((η^6-C_6H_5)C_5Ph_4H)]Cl and [Fe(η^5-C_5Ph_5)((η^6-C_6H_5)C_5Ph_4H)]F are much more soluble than their unprotonated forms [Fe(η^5-C_5Ph_5)((η^6-C_6H_5)C_5Ph_4)]Cl and [Fe(η^5-C_5Ph_5)((η^6-C_6H_5)C_5Ph_4)]F. This explanation is consistent with the observation made in the electrochemical experiments of [Fe(η^5-C_5Ph_5)((η^6-C_6H_5)C_5Ph_4H)]BF_4 in 0.1 M NaCl electrolyte solution (see above). An analogous result was obtained when 0.1 M NaF was the electrolyte. It is also probable that dissolution of [Fe(η^5-C_5Ph_5)((η^6-C_6H_5)C_5Ph_4H)]Cl and [Fe(η^5-C_5Ph_5)((η^6-C_6H_5)C_5Ph_4H)]F occurs prior to protonation, as the redox couple [Fe(η^5-C_5Ph_5)((η^6-C_6H_5)C_5Ph_4H)]$^{+/0}$ is either very weak (with Cl^- as the anion) or not detected (with F^- as the anion). If dissolution occurs, then protonation may occur in the bulk solution rather than at the electrode−solid interface, and hence [Fe(η^5-C_5Ph_5)((η^6-C_6H_5)C_5Ph_4H)]$^+$ will not be voltammetrically detected in its very dilute solution-phase concentration. Data obtained with the different electrolytes are summarized in Table 1.

(ii) Processes at Very Positive Potentials. Extension of the potential range to more positive potentials of 1200 mV with 0.1 M $NaClO_4$ as the electrolyte reveals two barely resolved chemically irreversible oxidation processes at 945 and 1040 mV. The charge-transfer process associated with the second oxidation step of Fe(η^5-C_5Ph_5)((η^6-C_6H_5)C_5Ph_4) (E_p^{ox} = 945 mV) is proposed to be

$$[Fe(\eta^5\text{-}C_5Ph_5)((\eta^6\text{-}C_6H_5)C_5Ph_4)]ClO_{4(solid)} + ClO_4^-{}_{(solution)} \rightleftharpoons [Fe(\eta^5\text{-}C_5Ph_5)((\eta^6\text{-}C_6H_5)C_5Ph_4)][ClO_4]_{2(solid)} + e^- \quad (7)$$

However, when cycling of the potential encompasses this second oxidation step, only a very weak wave for reduction of [Fe(η^5-C_5Ph_5)((η^6-C_6H_5)C_5Ph_4)]ClO_4 is observed even on the initial reverse potential direction scan. Instead, the [Fe(η^5-C_5Ph_5)((η^6-C_6H_5)C_5Ph_4H)]$^{+/0}$ redox couple is immediately present as a major process on this initial reverse scan and in all subsequent cycles (Figure 3c). Furthermore, in contrast to the experiments in the narrower potential range, the weak irreversible reduction wave observed in the voltammetry of [Fe(η^5-C_5Ph_5)((η^6-C_6H_5)C_5Ph_4H)]ClO_4 (Figure 1) is visible in the potential region of around −500 mV (Figure 3c).

The almost instantaneous formation of the protonated compound [Fe(η^5-C_5Ph_5)((η^6-C_6H_5)C_5Ph_4H)]$^+$ when scanning to very positive potentials implies a reaction involving the oxidation of water. Thus, for example the overall process

$$2[Fe(\eta^5\text{-}C_5Ph_5)((\eta^6\text{-}C_6H_5)C_5Ph_4)]^{2+}{}_{(solid)} + 2H_2O \rightarrow 2[Fe(\eta^5\text{-}C_5Ph_5)((\eta^6\text{-}C_6H_5)C_5Ph_4H)]^+{}_{(solid)} + O_{2(solution)} + 2H^+{}_{(solution)} \quad (8)$$

Table 3. Cyclic Voltammetric Data[a] Associated with the Second and Third Oxidation Processes for Fe(η^5-C_5Ph_5)((η^6-C_6H_5)C_5Ph_4) Mechanically Attached to Basal Plane Pyrolytic Graphite Electrode Immersed in a (70:30) Water/Acetonitrile (0.1 M Electrolyte) Solvent Mixture

	0.1 M electrolyte[b]				
	$NaClO_4$ (7.2)	$HClO_4$ (1.0)	KBF_4 (5.0)	NaCl (6.4)	NaF (7.7)
E_p^{ox} (mV)[c]	945	960	975	970	1080
E_p^{ox} (mV)[d]	1040	1040	1110	1050	1235

[a] $T = 20 \pm 2$ °C, scan rate = 200 mV s^{-1}, potentials reported versus Ag/AgCl (3 M NaCl). [b] "pH-values" of the electrolyte are in parentheses. [c] Second oxidation process. [d] Third oxidation process.

may occur to produce the protonated species. However, oxygen has not been identified as a reaction product so that alternative radical reaction pathways also may be involved in the conversion of [Fe(η^5-C_5Ph_5)((η^6-C_6H_5)C_5Ph_4)]$^{2+}_{(solid)}$ to [Fe(η^5-C_5Ph_5)((η^6-C_6H_5)C_5Ph_4H)]$^{+}_{(solid)}$. With the other electrolytes considered, two weak oxidation steps also are observed in the potential region of 945 to 1235 mV (Table 3). This time, in contrast to the narrower potential scan range experiments, the formation of Fe(η^5-C_5Ph_5)((η^6-C_6H_5)C_5Ph_4H) can be detected with 0.1 M NaCl and NaF as the electrolyte after encompassing the second oxidation process.

Further extension of the potential to 1400 mV in the positive direction produces a strong oxidation peak around 1350 mV in all electrolytes. This value is comparable with the oxidation potential obtained for the oxidation of [Fe(η^5-C_5Ph_5)((η^6-C_6H_5)C_5Ph_4H)]$^+$ (see above). Again, upon continuous cycling several other reduction and oxidation waves are visible in the reverse scan and subsequent cycles in addition to those for the reduction and reoxidation of [Fe(η^5-C_5Ph_5)((η^6-C_6H_5)C_5Ph_4H)]$^+$. The peak currents for the [Fe(η^5-C_5Ph_5)((η^6-C_6H_5)C_5Ph_4H)]$^{+/0}$ redox couple decrease with cycling, while the peak currents for the new waves increase in the second and third cycle, but then slowly disappear with further cycling, presumably because of dissolution of the products formed. In the second cycle, the strong oxidation peak at $E_p^{ox} = 1350$ mV is no longer observed.

Voltammetry of Microcrystals of HC_5Ph_5 Mechanically Attached to a Graphite Electrode Placed in (70:30) Water/Acetonitrile (0.1 M Electrolyte). HC_5Ph_5 is closely related to part of the ligand system in [Fe(η^5-C_5Ph_5)((η^6-C_6H_5)C_5Ph_4H)]$^+$. Voltammetric oxidation of the organic moiety HC_5Ph_5 mechanically attached to a basal plane pyrolytic graphite electrode immersed in the mixed solvent (0.1 M $NaClO_4$) occurs at very positive potential ($E_p^{ox} = 1370$ mV). The peak potential for this irreversible process is similar to that observed for the irreversible oxidation of [Fe(η^5-C_5Ph_5)((η^6-C_6H_5)C_5Ph_4H)]BF_4 (1355 mV, Figure 2) and the fourth oxidation process for [Fe(η^5-C_5Ph_5)((η^6-C_6H_5)C_5Ph_4)] (1350 mV), implying that the latter two processes are ligand rather than metal based. The oxidation peak for HC_5Ph_5 is not evident during the second cycle, implying that the cation $[HC_5Ph_5]^+$ is either unstable or dissolves from the electrode surface under the experimental conditions. Additionally, small irreversible reduction and oxidation processes emerge in the second and third cycles at $E_p^{red} = -620$, -1090, and -1450 mV and $E_p^{ox} = 630$, 930, and 1130 mV (Table 2), which then slowly diminish with further cycling. The oxidation process at 1130 mV was observed when a larger amount of HC_5Ph_5 was attached to the electrode surface. These peak potentials for these processes are comparable with those for the processes that emerge in the second cycle when [Fe(η^5-C_5Ph_5)((η^6-C_6H_5)C_5Ph_4H)]BF_4 and [Fe(η^5-C_5Ph_5)((η^6-C_6H_5)C_5Ph_4)] (fourth process) are oxidized (Table 2).

Electrospray Mass Spectrometric (ESMS) Studies. Voltammetric results of solid-state experiments imply that solid Fe(η^5-C_5Ph_5)((η^6-C_6H_5)C_5Ph_4) in contact with water slowly converts to the protonated cation [Fe(η^5-C_5Ph_5)((η^6-C_6H_5)C_5Ph_4H)]$^+$ according to eq 6 (see above). Additionally, results imply that the compound may be oxidized to [Fe(η^5-C_5Ph_5)((η^6-C_6H_5)C_5Ph_4)]$^+$ on the voltammetric time scale. The cations formed via redox or protonation reactions can be identified by the ESMS method.

After 50 min of bulk electrolysis at a potential of 600 mV of solid Fe(η^5-C_5Ph_5)((η^6-C_6H_5)C_5Ph_4) attached to a pyrolytic graphite electrode placed in contact with 0.1 M $NaClO_4$ as the electrolyte, the solid was dissolved in acetonitrile. ES mass spectra of this solution gave an *m/e* value of 947. Simulation of the mass spectrum shows that the observed isotopic pattern and this *m/e* value correspond to those expected from formation of [Fe(η^5-C_5Ph_5)((η^6-C_6H_5)C_5Ph_4H)]$^+$. A control experiment, where a sample of solid [Fe(η^5-C_5Ph_5)((η^6-C_6H_5)C_5Ph_4H)]BF_4 attached to a pyrolytic graphite electrode surface was placed for 2 min into a (70:30) water/acetonitrile (electrolyte) solution at an open circuit potential prior to the ESMS experiment, gave the same ES mass spectrum. However, when bulk electrolysis of Fe(η^5-C_5Ph_5)((η^6-C_6H_5)C_5Ph_4) is stopped after only 10 min, the ESMS experiment of solid dissolved in acetonitrile produced a complex overlapping spectrum which could be assigned to the formation of two cations, [Fe(η^5-C_5Ph_5)((η^6-C_6H_5)C_5Ph_4)]$^+$ (*m/e* = 946) and [Fe(η^5-C_5Ph_5)((η^6-C_6H_5)C_5Ph_4H)]$^+$ (*m/e* = 947). Apparently the [Fe(η^5-C_5Ph_5)((η^6-C_6H_5)C_5Ph_4)]$^+$ cation initially formed by bulk oxidative electrolysis also is slowly converted to [Fe(η^5-C_5Ph_5)((η^6-C_6H_5)C_5Ph_4H)]$^+$ via either of the overall reactions

$$2[Fe(\eta^5\text{-}C_5Ph_5)((\eta^6\text{-}C_6H_5)C_5Ph_4)]^+_{(solid)} + 2H_2O \rightarrow 2[Fe(\eta^5\text{-}C_5Ph_5)((\eta^6\text{-}C_6H_5)C_5Ph_4H)]^+_{(solid)} + H_2O_{2(solution)} \quad (9)$$

or

$$4[Fe(\eta^5\text{-}C_5Ph_5)((\eta^6\text{-}C_6H_5)C_5Ph_4)]^+_{(solid)} + 2H_2O \rightarrow 4[Fe(\eta^5\text{-}C_5Ph_5)((\eta^6\text{-}C_6H_5)C_5Ph_4H)]^+_{(solid)} + O_2 \quad (10)$$

As is the case with conversion of [Fe(η^5-C_5Ph_5)((η^6-C_6H_5)C_5Ph_4)]$^{2+}_{(solid)}$ to [Fe(η^5-C_5Ph_5)((η^6-C_6H_5)C_5Ph_4H)]$^{+}_{(solid)}$ (eq 8 and related discussion), no oxygen-containing species have been identified as reaction products, so that radical-based reaction pathways also could be associated with the conversion of [Fe(η^5-C_5Ph_5)((η^6-C_6H_5)C_5Ph_4)]$^{+}_{(solid)}$ to [Fe(η^5-C_5Ph_5)((η^6-C_6H_5)C_5Ph_4H)]$^{+}_{(solid)}$. A reaction of this kind probably also contributes to the voltammetry when long time scale redox cycling experiments are undertaken as catalysis

of the reaction is observed relative to the spontaneous reaction that occurs very slowly at open circuit potentials. The presence of the protonation reaction of Fe(η^5-C_5Ph_5)((η^6-C_6H_5)C_5Ph_4) to [Fe(η^5-C_5Ph_5)((η^6-C_6H_5)C_5Ph_4H)]$^+$ observed in the electrochemical experiments without oxidizing Fe(η^5-C_5Ph_5)((η^6-C_6H_5)C_5Ph_4) (eq 6) was also confirmed by an ESMS experiment. A sample of solid Fe(η^5-C_5Ph_5)((η^6-C_6H_5)C_5Ph_4) was attached to a pyrolytic graphite electrode surface and placed into a (70:30) water/acetonitrile (electrolyte) solution at an open circuit potential. After 50 min the electrode surface was carefully rinsed with water and the solid dissolved in acetonitrile. The ESMS experiment showed the expected *m/e* value of 947 and the isotopic pattern for the [Fe(η^5-C_5Ph_5)((η^6-C_6H_5)C_5Ph_4H)]$^+$ cation, confirming that the spontaneous protonation of Fe(η^5-C_5Ph_5)((η^6-C_6H_5)C_5Ph_4) occurs according to eq 6.

Electrochemical Quartz Crystal Microbalance (EQCM) Studies on Solid Fe(η^5-C_5Ph_5)((η^6-C_6H_5)-C_5Ph_4) and [Fe(η^5-C_5Ph_5)((η^6-C_6H_5)C_5Ph_4H)]BF_4 (i) Fe(η^5-C_5Ph_5)((η^6-C_6H_5)C_5Ph_4). Figure 4a illustrates the first five voltammetric cycles and the corresponding mass change data (assuming that the Sauerbrey equation[14] is valid, which requires that the solid is rigidly attached to the electrode at all times) obtained at a scan rate of 50 mV s^{-1} over a potential range of 0 to 800 mV for the oxidation of solid Fe(η^5-C_5Ph_5)((η^6-C_6H_5)C_5Ph_4) mechanically attached to a gold electrode in (70:30) water/acetonitrile (0.1 M $NaClO_4$). Interestingly, the peak heights associated with the [Fe(η^5-C_5Ph_5)((η^6-C_6H_5)C_5Ph_4)]$^{+/0}$ redox couple now decrease very rapidly in the first two cycles under these EQCM conditions, so that from the third cycle onward the [Fe(η^5-C_5Ph_5)-((η^6-C_6H_5)C_5Ph_4)]$^{+/0}$ redox couple is observed only as a very weak response. In the corresponding mass versus potential measurement the mass increases at a potential of 350 mV when oxidation to generate [Fe(η^5-C_5-Ph_5)((η^6-C_6H_5)C_5Ph_4)]$^+$ is accompanied by the uptake of the perchlorate anion to maintain electroneutrality. Under the conditions of the experiment shown in Figure 4a, the mass increase in the first cycle is 764 ng, whereas the mass decrease on the reverse scan due to reduction and concomitant expulsion of the perchlorate anion from the solid is only 275 ng. This decrease corresponds to 31% of the mass increase, implying that another reaction is occurring during the course of redox cycling in the positive potential region. The mass change associated with the perchlorate anion uptake and loss from solid decreases rapidly until the mass change is almost constant from the fourth (197 ng) to the fifth cycle (194 ng).

Cycling in the negative potential region from −400 to −1100 mV under EQCM conditions confirms that a significant quantity of the protonated species has been formed spontaneously (Figure 4b, cycles 6−10) and that this process contributes to the time and scan rate dependent mass changes shown in Figure 4a. The protonation of Fe(η^5-C_5Ph_5)((η^6-C_6H_5)C_5Ph_4) under EQCM conditions is very fast in contrast to the stationary basal plane pyrolytic graphite or gold electrode experiment, where many cycles were necessary to achieve a "steady-state" voltammetric response. This difference possibly

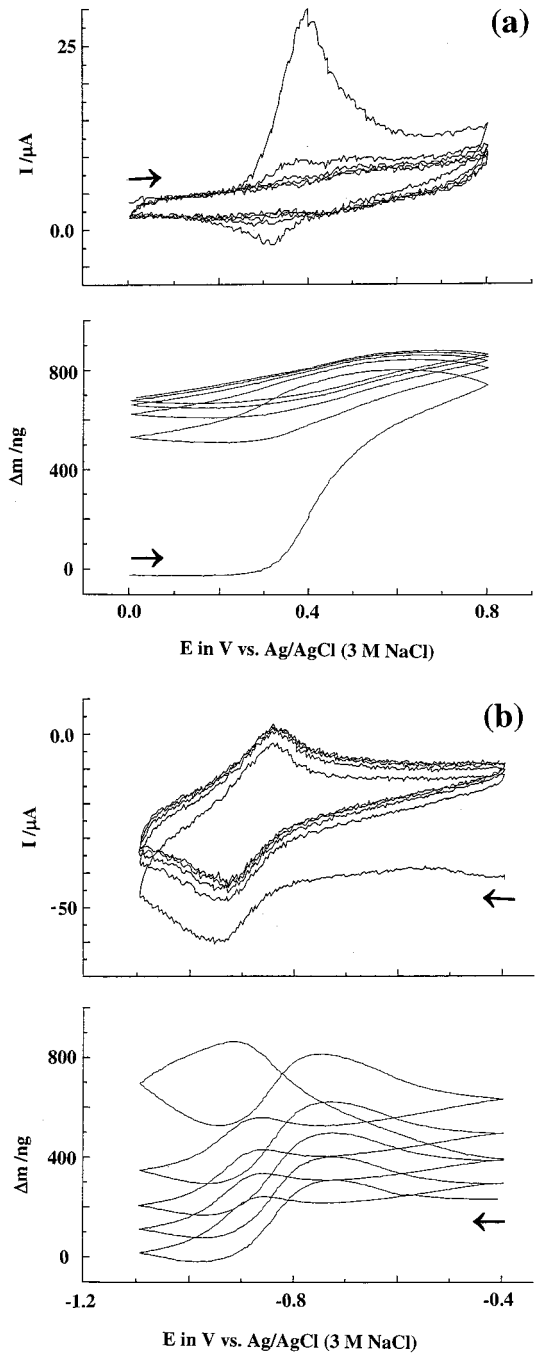

Figure 4. Cyclic voltammograms (upper curves) and EQCM mass-potential data (lower curves) obtained at a scan rate of 50 mV s^{-1} for Fe(η^5-C_5Ph_5)((η^6-C_6H_5)C_5Ph_4) mechanically attached to a gold-coated quartz crystal electrode placed in (70:30) water/acetonitrile (0.1 M $NaClO_4$): (a) cycles 1−5 and (b) cycles 6−10.

occurs because the vibration of the quartz crystal enhances the rate of transport of protons across the solid−solution interface with presumably the rates of the reaction in eqs 6 and 9 (or 10) all being enhanced. However, the fact that the constant mass change, the weakly observed [Fe(η^5-C_5Ph_5)((η^6-C_6H_5)C_5Ph_4)]$^{+/0}$ redox couple, and the voltammetric "steady state" is reached after five cycles (Figure 4a) confirm that an equilibrium between Fe(η^5-C_5Ph_5)((η^6-C_6H_5)C_5Ph_4) and [Fe(η^5-C_5-Ph_5)((η^6-C_6H_5)C_5Ph_4H)]$^+$ is rapidly established at the vibrating electrode according to eq 6. The net mass increase measured at the initial potential when the

(14) Ward, M. D. In *Physical Electrochemistry*; Rubinstein, I., Ed.; Marcel Dekker: New York, 1995.

potential is scanned as in Figure 4a therefore effectively corresponds to the uptake of protons to form the cation and to the uptake of the perchlorate anion which is needed to achieve electroneutrality when [Fe(η^5-C_5Ph_5)-((η^6-C_6H_5)C_5Ph_4H)]ClO_4 is formed.

The reduction and reoxidation of [Fe(η^5-C_5Ph_5)((η^6-C_6H_5)C_5Ph_4H)]ClO_4 formed under EQCM conditions during the course of the experiment depicted in Figure 4a and the corresponding mass change detected in the potential range from −400 to −1100 mV are shown in Figure 4b (cycles 6−10). The discontinuity in data between the two data sets in Figure 4a,b is a result of the time taken to alter the experimental conditions. At the potential of −900 mV, where the reduction of [Fe-(η^5-C_5Ph_5)((η^6-C_6H_5)C_5Ph_4H)]ClO_4 occurs (Figure 4b), a decrease of mass is detected which corresponds to the expulsion of the perchlorate anion. When the uncharged complex is formed at the electrode surface, the reoxidation of Fe(η^5-C_5Ph_5)((η^6-C_6H_5)C_5Ph_4H) at around −850 mV is accompanied by the mass increase associated with the uptake of the perchlorate anion. However, the mass increase associated with the uptake of the perchlorate anion on the reverse scan (oxidation) is bigger than the mass decrease attributed to the expulsion of the counterion on the forward scan (reduction). Furthermore, at potentials prior to the reduction of [Fe(η^5-C_5Ph_5)((η^6-C_6H_5)C_5Ph_4H)]ClO_4 a mass increase occurs, and at potentials after reoxidation of Fe(η^5-C_5Ph_5)((η^6-C_6H_5)C_5-Ph_4H) a mass decrease is observed. The latter two forms of change in mass diminish with cycling of the potential.

The mass increase prior to the main reduction process diminishes with cycling and may be related to the process observed in this potential region in the voltammetric experiments at the stationary graphite electrode (see above discussion and data in Table 1).

On continuous cycling of the potential, the net mass of solid attached to the electrode determined at the initial potential slowly decreases either because of a slight dissolution or mechanical loss of one form of the solid from the vibrating electrode or because of reconversion of [Fe(η^5-C_5Ph_5)((η^6-C_6H_5)C_5Ph_4H)]ClO_4 to the unprotonated form (see below).

(ii) [Fe(η^5-C_5Ph_5)((η^6-C_6H_5)C_5Ph_4H)]BF_4. The reduction of [Fe(η^5-C_5Ph_5)((η^6-C_6H_5)C_5Ph_4H)]BF_4 mechanically attached to a vibrating gold electrode under EQCM conditions over a potential range of −200 to −1100 mV in (70:30) water/acetonitrile (0.1 M $NaClO_4$) and with a scan rate of 50 mV s^{-1} also was studied for 5 cycles of the potential. In the voltammetry, the reduction and oxidation peaks for the [Fe(η^5-C_5Ph_5)((η^6-C_6H_5)C_5-Ph_4H)]$^{+/0}$ redox couple are observed as in Figure 4b together with a broad process over the potential range prior to this process. Both the current magnitudes for the broad process at −550 mV and those associated with the [Fe(η^5-C_5Ph_5)((η^6-C_6H_5)C_5Ph_4H)]$^{+/0}$ redox couple decrease upon cycling. The latter feature is as expected on the basis of data obtained from the experiments with the basal plane pyrolytic graphite electrode when it was shown that spontaneous conversion to the deprotonated form occurs until an equilibrium position is reached. The potential−mass change data are slightly more complicated than those obtained when a relatively low coverage of [Fe(η^5-C_5Ph_5)((η^6-C_6H_5)C_5Ph_4H)]ClO_4 was formed by conversion from Fe(η^5-C_5Ph_5)((η^6-C_6H_5)C_5Ph_4) (Figure 4b), but still exhibit the same main features. Thus, in the potential region of around −900 mV the mass initially decreases (reduction process) because of the release of the perchlorate anion into the solution and then increases due to the incorporation of the perchlorate anion (oxidation process). However, in contrast to the experiment with [Fe(η^5-C_5Ph_5)((η^6-C_6H_5)C_5Ph_4H)]-ClO_4 formed from Fe(η^5-C_5Ph_5)((η^6-C_6H_5)C_5Ph_4) (see above), the net mass at the initial potential decreases during the course of each reduction−oxidation cycle.

The substantial mass increase at potentials prior to the reduction of [Fe(η^5-C_5Ph_5)((η^6-C_6H_5)C_5Ph_4H)]ClO_4 in the initial cycle again is associated with the broad irreversible process observed in the voltammetry, although part of the net mass change also may be associated with the exchange of the tetrafluoroborate and perchlorate anions and there may be other nonvoltammetrically detected responses contributing to the mass change.

The initial 5 cycles of voltammograms obtained in the positive potential region confirm that some of the [Fe-(η^5-C_5Ph_5)((η^6-C_6H_5)C_5Ph_4H)]ClO_4 has been spontaneously converted to the unprotonated Fe(η^5-C_5Ph_5)((η^6-C_6H_5)C_5Ph_4) form. As expected, this form of the compound is again rapidly protonated on redox cycling of the potential within the second five cycles. Voltammograms and corresponding features in the mass changes measured for Fe(η^5-C_5Ph_5)((η^6-C_6H_5)C_5Ph_4) and the reprotonated [Fe(η^5-C_5Ph_5)((η^6-C_6H_5)C_5Ph_4H)]ClO_4 are similar to those described above. The fast deprotonation of Fe(η^5-C_5Ph_5)((η^6-C_6H_5)C_5Ph_4H) and protonation of Fe-(η^5-C_5Ph_5)((η^6-C_6H_5)C_5Ph_4) in these experiments presumably occur at a much greater rate than is the case at a stationary graphite or gold electrode because of the vibration of the quartz crystal. That is, the rates of reaction given by eqs 5, 6, and 9 (or 10) have all increased.

Finally, it should be noted that the validity of the Sauerbrey equation under the above conditions when the nature of the solid attached to the electrode surface is occurring via a range of reactions is uncertain. Consequently, quantitative interpretation of the mass change data accompanying the voltammetry is unwarrented.

Conclusions

Voltammetric, ESMS and EQCM data confirm that interconversion of [Fe(η^5-C_5Ph_5)((η^6-C_6H_5)C_5Ph_4H)]$^+$ and Fe(η^5-C_5Ph_5)((η^6-C_6H_5)C_5Ph_4) may be achieved by either altering the "pH" at the solid−solvent (electrolyte) interface or via redox processes occurring at a solid−electrode−solvent (electrolyte) interface. Results on the solids complement those previously obtained in the solution phase.[13]

Acknowledgment. The authors thank the Ciba-Geigy Jubiläumsstiftung [A.L.] and the Australian Research Council for their financial support of this project. The provision of samples of Fe(η^5-C_5Ph_5)((η^6-C_6H_5)C_5Ph_4) and [Fe(η^5-C_5Ph_5)((η^6-C_6H_5)C_5Ph_4H)]BF_4 by A. F. Masters and extensive discussions with F. Marken also are gratefully acknowledged.

OM9807553